

Stochastic Simulation of Human Pulmonary Blood Flow and Transit Time Frequency Distribution Based on Anatomic and Elasticity Data

Wei Huang*, Jun Shi[†] and R. T. Yen^{†‡}

Abstract: The objective of our study was to develop a computing program for computing the transit time frequency distributions of red blood cell in human pulmonary circulation, based on our anatomic and elasticity data of blood vessels in human lung. A stochastic simulation model was introduced to simulate blood flow in human pulmonary circulation. In the stochastic simulation model, the connectivity data of pulmonary blood vessels in human lung was converted into a probability matrix. Based on this model, the transit time of red blood cell in human pulmonary circulation and the output blood pressure were studied. Additionally, the stochastic simulation model can be used to predict the changes of blood flow in human pulmonary circulation with the advantage of the lower computing cost and the higher flexibility. In conclusion, a stochastic simulation approach was introduced to simulate the blood flow in the hierarchical structure of a pulmonary circulation system, and to calculate the transit time distributions and the blood pressure outputs.

Keywords: capillary sheet, connectivity matrix, Diameter-Defined Strahler System, steady blood flow, transit time frequency distribution.

1 Introduction

Human pulmonary blood flow plays important roles in gas exchange, mechanotransduction [Chiu and Chien (2011)], and the diseases of the lung and heart [Yuan, Garcia, Hales, Stuart, Archer and West (2010)]. Although modern technologies have been applied to study the complex blood flow and transit time in human lung [MacNee, Martin, Wiggs, Belzberg, Hogg (1989); Lewis, Caterinam, Giuntini, (1994); Hopkins, Belzbergm, Wiggson, McKenzie (1996); Zavorsky, Walley, Russell (2003)], a thorough theoretical understanding with full experimental

* Dept. of Mechanical Engineering, Hong Kong University of Science and Technology, Clear Water Bay, Kowloon, Hong Kong

[†] Dept. of Biomedical Engineering, University of Memphis, Memphis, TN 38152

[‡] Correspondent author. E-mail: myen@memphis.edu.

verification is essential [Tawhai, Clark, Burrowes (2011)]. A significant approach to analyze such complicated network is to characterize the transit time distribution in pulmonary circulation [Fung (1996)].

The lung handles the oxygenation of the blood. The carriers of the oxygen are the red blood cells. Pulmonary transit time is defined as the length of time it takes for a red blood cell to travel through the pulmonary circulation. Different cells take different paths in traveling. Theoretically, transit times vary from streamline to streamline. In analogy to the statistical distribution of a random variable, the transit time distribution of a given lung is defined as a frequency function of the transit time, denoted as $f(t)$, for which $f(t)dt$ is equal to the fraction of the fluid that enters the lung whose transit time lies between t and $t+dt$ [Fung, YC (1996)]. The pulmonary circulation system can be considered as a distributed network of vessels of various lengths and diameters. The distributions of pulmonary transit time reflect perfused vascular volume and contact time between blood and vascular surface area, both of which affect gas exchange and metabolic functions of the pulmonary endothelium. In the lung, the red cells spread into a vast sheet of capillaries. By applying the sheet flow theory [Fung and Sobin (1969)], the theoretical transit time distributions in the pulmonary capillary sheet were calculated [Fung and Sobin (1972)].

In our group, the idea of statistical sampling was introduced in [McLaurine (1997)]. The frequency distributions of the pulmonary arterial and venous trees and the capillary sheet were convoluted together to obtain the total transit time for the pulmonary circulation [McLaurine (1997)]. Later on, a complex arterial network model close to the real arterial system in terms of size and topology was constructed [Zhou (2005)]. Gravity flow algorithm was used to solve the network flow problem, which produced the maximum flow in a flow network with segments of different sizes, accompanied with the method of back propagation training [Zhou (2005)]. However, in these sophisticated computer algorithms [McLaurine (1997); Zhou (2005)], the size of data in pulmonary circulation system became too big to be handled even by a super computer.

In the present paper, a stochastic simulation model was introduced to simulate steady blood flow in human pulmonary circulation, based on our anatomic and elasticity data of blood vessels in human lung, which were summarized in [Huang, Zhou, Gao, Yen (2011)], and by converting the connectivity data of pulmonary blood vessels in human lung [Huang, Yen, McLaurine, Bledsoe (1996)] into a probability matrix. Based on the present model, the transit time frequency distributions of red blood cell in human pulmonary circulation and the output blood pressure were studied.

2 Methodologies

2.1 Morphometric and elastic property of human lung

By measuring the silicone elastomer casts of human pulmonary blood vessels, the pulmonary vasculature system was constructed, which consists of 15 orders of arteries between the main pulmonary artery and capillary sheet and 15 orders of veins between the capillary sheet and left atrium [Huang, Yen, McLaurine and Bledsoe (1996)]. The diameter-defined Strahler ordering model [Kassab, Rider, Tang, Fung (1993)] was used to assign branching orders. Two connectivity matrixes for describing the connection of blood vessels from one order to another in arterial and venous trees, respectively, were obtained [Huang, Yen, McLaurine and Bledsoe (1996)]. The data for vessels includes apparent viscosity of the blood and compliance, which were collected from different sources, were summarized in Tables 1-3 in [Huang, Zhou, Gao, Yen (2011)].

2.2 Pressure-flow relation in steady flow condition

2.2.1 Pressure-flow relation of arteries and veins in steady flow condition

In the present work, the mathematical approach of pressure-flow analysis in steady flow used is similar to that of [Zhuang, Fung and Yen (1983)]. A brief description is given below. The vessel diameter D changes linearly with the appropriate transmural pressure ΔP in pulmonary arteries and veins,

$$\frac{D}{D_0} = 1 + \beta \Delta P, \quad (1)$$

where D_0 is the tube diameter when transmural pressure is zero and β is the compliance coefficient of the vessel wall defined in [Yen, Fung, Bingham (1980)]. For a viscous incompressible fluid in vessel tube, the steady flow is governed by Poiseuille's law and can be presented in the fifth power law as

$$\frac{640\mu\beta D_0 L}{\pi} \dot{Q} = D_0^5 \left[(1 + \beta \Delta P_{entry})^5 - (1 + \beta \Delta P_{exit})^5 \right] \quad (2)$$

where μ is the apparent viscosity of blood, L is the length of the vessel, \dot{Q} is the flow rate in the vessel, ΔP_{entry} and ΔP_{exit} are transmural pressures at the entry and exit ends of the vessel [Fung (1996)].

When applying Eq. (2) in computation, ΔP is calculated as follows cmH₂O. For pulmonary vessels with diameters much larger than the alveolar diameter and smaller than the alveolar diameter, we have Eq. (3) and (4), respectively,

$$\Delta P = P - P_{pl}, \quad (3)$$

$$\Delta P = P - P_A, \tag{4}$$

where P is blood pressure, P_A is airway pressure and P_{pl} is pleural pressure.

2.2.2 *Pressure-flow relation of capillary sheet in steady flow condition*

In the sheet flow theory [Fung and Sobin (1969)], the dense network of capillaries in pulmonary alveolar wall is modeled as a sheet of fluid flowing between two membranes held apart by a large number of regularly spaced posts. If the local blood pressure P is larger than the alveolar gas pressure P_A , then the capillary sheet thickness can be derived by

$$h = h_0 + \alpha(P - P_A), \tag{5}$$

where h is the sheet thickness, h_0 is the thickness of capillary sheet at zero pressure difference when the pressure decreases from positive values, α is the compliance constant of the capillary sheet. Based on Eq. (5), the pressure-flow relationship in capillary sheet is derived as [Fung and Sobin (1972)]

$$\dot{Q} = const (h_a^4 - h_v^4) = const \left\{ [h_0 + \alpha(P_{art} - P_A)]^4 - [h_0 + \alpha(P_{ven} - P_A)]^4 \right\}, \tag{6}$$

where \dot{Q} is the volume flow rate, h_a is the sheet thickness at the arteriole end, h_v is the sheet thickness at the venule end, and P_{art} and P_{ven} are pressures at the corresponding arteriole and venule. The constant *const* is

$$\frac{SA}{4\mu k f \bar{L}^2 \alpha}, \tag{7}$$

where A is alveolar area, S is the vascular-space-tissue ratio, representing the fraction of the blood volume over a sum of the volumes of the vascular space and the posts. μ is the apparent viscosity of blood in the capillary sheet. k and f are dimensionless factors which describe alveolar structural geometry. \bar{L} is the average length of streamlines between an arteriole and a venule.

Equations (5) and (6) are valid only when $P_{ven} \geq P_A$. If $P_{ven} < P_A$, it is said to be in zone 2 condition and “waterfall” occurs. The sluicing gate is located at the junction of the capillary sheet and its draining venule. Hence in zone 2 condition h_v tends to 0, and the flow depends only on h_a .

In the present study, losses due to turbulence and bifurcation are ignored. A repeated application of Eq. (2) to each order of pulmonary arteries and veins as well as the application of Eq. (6) to the capillary sheet make a complete pulmonary circulation system.

2.3 Probability matrixes

In a simulating perspective, a pulmonary circulation includes the arterial tree where the blood flows from top (i.e., the pulmonary arterial trunk) to bottom (i.e., the smallest arteries), the pulmonary sheet which is similar to a traffic network, and the venous tree where the blood flows from bottom (i.e., the smallest veins) to top (i.e., the largest veins). The pulmonary circulation system can be considered as a distributed network of vessels of various lengths and diameters. We assume there is an independent blood particle traveling through the whole network. At every bifurcation, the blood cell has to determine which vessel to travel through by flow mechanism. If the blood cell travels enough times in the system, we can measure the transit time distribution statically viewpoint.

Two connectivity matrixes, which define the branching pattern of human pulmonary arteries and veins, respectively, were provided in [Huang, Yen, McLaurine, Bledsoe (1996)]. Both are two-dimensional matrices. MaxOrder is the maximal order for the arterial tree and the venous tree, i.e., 15×15 . The elements of the connectivity matrix are defined as the number of branches statistically coming from the upper level branches. For example, $CM(i, j)$ means the number of branches at the level j can be generated from one branch at the level i . Let us use $P(i, j)$ for the probability that a branch at the level i will lead to a branch at the level j . Mathematically it can be expressed in the following equation:

$$P(i, j) = CM(i, j) / \sum \{CM(i, j), j\} \quad (8)$$

Assume the blood cell starts the trip from the branch 1, it may lead to the branch with the probability of $P(1, 1)$. It may lead to the branch 2 with the probability of $P(1, 2)$. Finally the blood cell will reach the final branch level, i.e. 15. Then the blood cell will pass through the pulmonary sheet. In the same approach, the blood cell will pick a certain route to finish the journey in the venous tree until it complete the circulation. Using the generated probability matrixes, a simulation can be developed to calculate the transit time and blood pressure distributions given certain conditions.

2.4 Transit time calculation

2.4.1 Calculate the exit pressure

The transit calculation includes two steps: exit pressure and transit time. The exit pressure in artery and vein can be generated based on Eq. (2). The computer codes (C++) are shown as the following. For pulmonary sheet, Eq. (6) can be used.

2.4.2 Calculate the transit time for one section of tube

The schematic drawing of a cylindrical elastic vessel tube is shown in **Figure 1**.

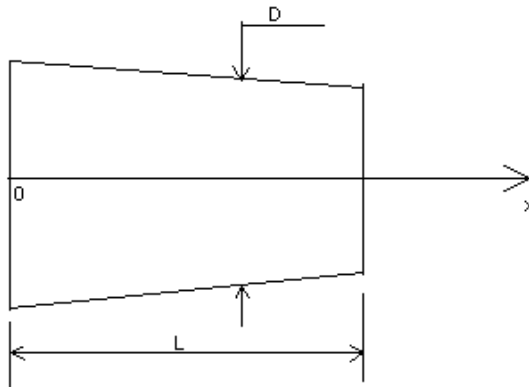


Figure 1: Schematic drawing of a cylindrical elastic vessel tube

The volume of this tube, V , can be derived as:

$$V = \int_0^L \frac{\pi D^2}{4} dx \tag{9}$$

where D is the diameter of this tube, and L is the length of this tube. Substituting Eq. (1) into Eq. (9), and applying the following boundary conditions:

$$P = P_{entry} \text{ for } x = 0, \quad P = P_{exit} \text{ for } x = L, \tag{10}$$

the following equation is obtained for volume V

$$V = \frac{\pi}{4} D_0^2 L \left(1 + \beta P_{entry} + \beta P_{exit} + \frac{1}{3} \beta^2 P_{entry}^2 + \frac{1}{3} \beta^2 P_{exit}^2 + \frac{1}{3} \beta^2 P_{entry} P_{exit} \right), \tag{11}$$

where L is the length of the vessel, ΔP_{entry} and ΔP_{exit} are transmural pressures at the entry and exit ends of the vessel, D_0 is the tube diameter when transmural pressure is zero, and β is the compliance coefficient of the vessel wall defined in [Yen, Fung, Bingham (1980)].

Once a red blood cell completes a whole trip in the above described journey, the transit time and pressure values are calculated. The values are called one sample. Hundreds and thousands of calculations can be used to confirm the distribution

patterns. Primitive experiments showed that it took less than 1 second to run one sampling even in a personal computer (1.0 GHz processor, 640 MB RAM). The later experiments also showed that when the sampling size reached 100, a stabilized distribution pattern could be obtained.

2.4.3 Transit time for capillary sheet

To simplify the analysis, the theoretical transit time distributions in pulmonary capillary sheet presented in [Fung (1996)] were applied in the present study.

2.4.4 Total pulmonary transit time

For example, in a random route, a blood cell travels the branching levels of 15-14-13-12-11-9-6-3-1 for arteries, capillary sheet, and branching levels of 1-3-5-9-11-12-14-15 for veins. All these steps need transit times of 271, 328, 469, 407, 408, 307, 281, 14, 34, 5260, 114, 249, 192, 112, 101, 138, 105, and 118 ms. Thus it took the blood cell a total of 8917 ms to travel through the whole pulmonary system. A flowchart of the computational methods is shown in Appendix.

3 Results

The results obtained from the computer programming can be seen in **Figures 2-4**. In **Figure 2** it can be seen that a peak frequency of 193 examples was obtained around 2300 ms.

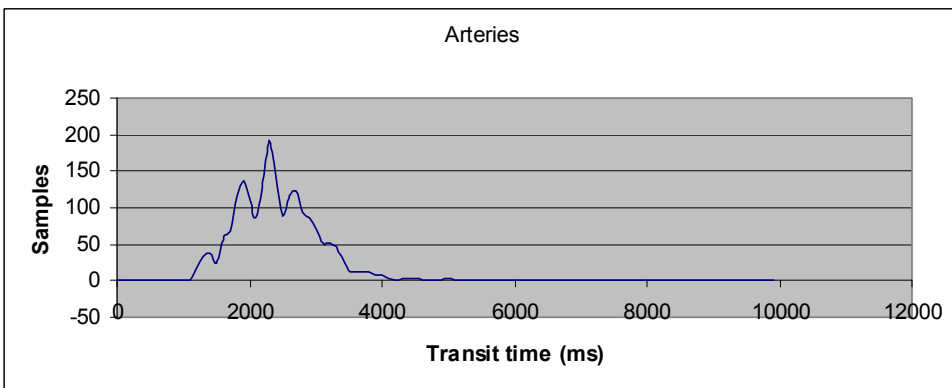


Figure 2: Distribution of transit time for arteries

The transit time in capillary sheet achieved a peak frequency of 448 at the transit time of 2000 ms as shown in **Figure 3**, and it had a distribution similar to what was

calculated in [Fung (1996)].

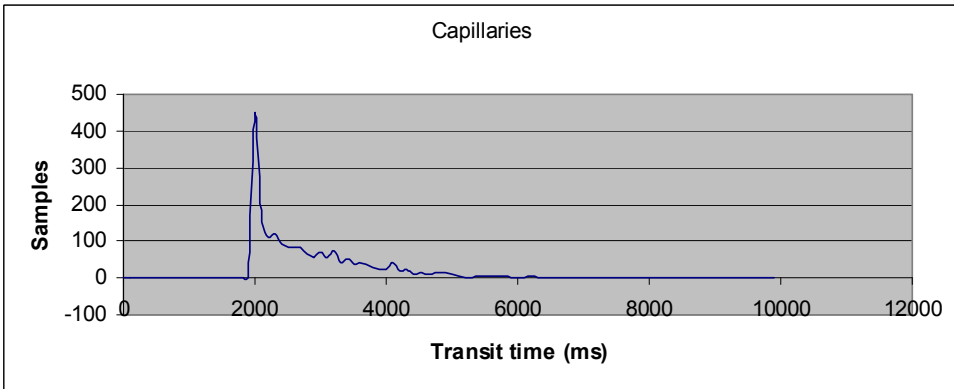


Figure 3: Distribution of transit time for capillary sheet

Then the distribution of the veins can be observed in **Figure 4**. The veins had a peak frequency of 193 at the transit time of 2000 ms. The veins had shorter average transit times. The distribution peak also more spread out than in arteries.

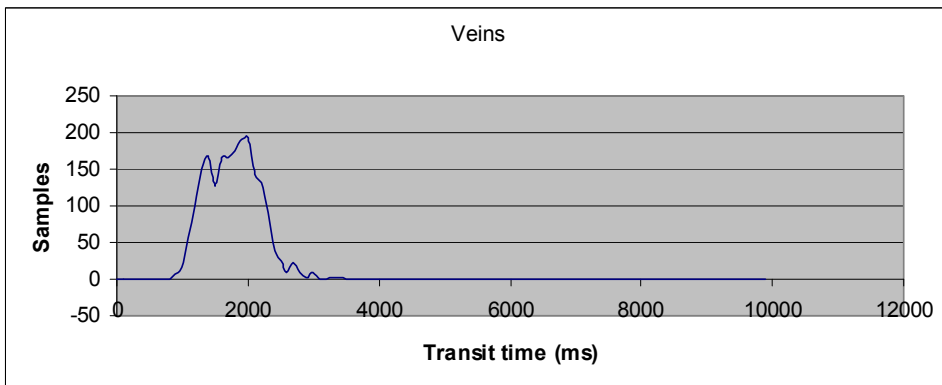


Figure 4: Distribution of transit time for veins

Overall the transit time distribution is shown in **Figure 5**. It has the peak frequency of 89 at the transit time of 6700 ms.

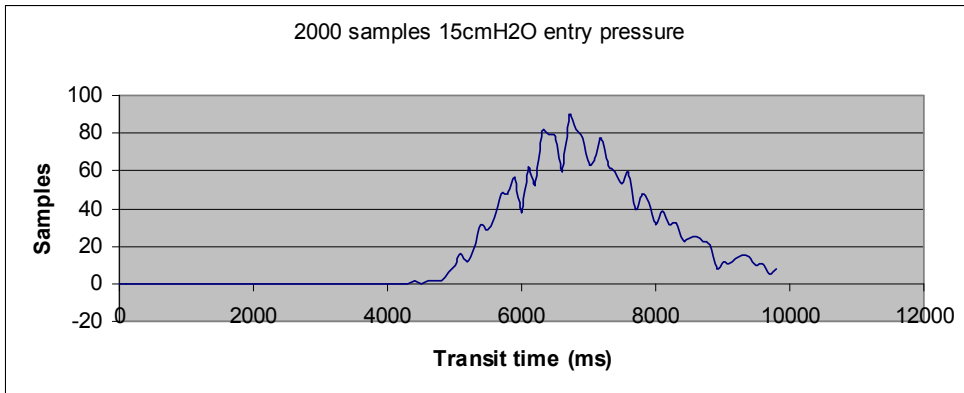


Figure 5: Distribution of transit time

4 Discussion

One assumption of the model is steady blood flow in the pulmonary circulation. All parameters used in the modeling remain constant while the pressure and flow change. The literature supports these assumptions, which hold true in a low pressure system like the pulmonary circulation.

Another assumption is the same order of the vessels share the same length, which means a linear branching system. In reality the vessel lengths are different. However, in the equation of the pressure-flow rate for the pulmonary system, the length is the first power while the diameter is the fifth power. The diameter is much more significant than the length. This issue is taken care of in the Diameter-Defined Strahler System which is applied in the present study.

In the present modeling method, there is no resistance at the branching intersections. Since there is little energy lost at the intersections in such a low pressure biological system, we assume there is no pressure and flow change at the branching points.

This stochastic simulation converges quickly. The defined curve for the transit time distribution for the whole pulmonary circulation is achieved when the sample size reaches 200. **Figure 6** shows how the distribution curves change when we increase the sample sizes from 1000 to 10000; however, the transit times for the peak frequency remain the same for different sample sizes.

The entry pressure is one of the key parameters which reflects the lung condition and are worth investigation. The results with different entry pressures are interesting. **Figure 7** shows the transit time distributions with different entry pressure

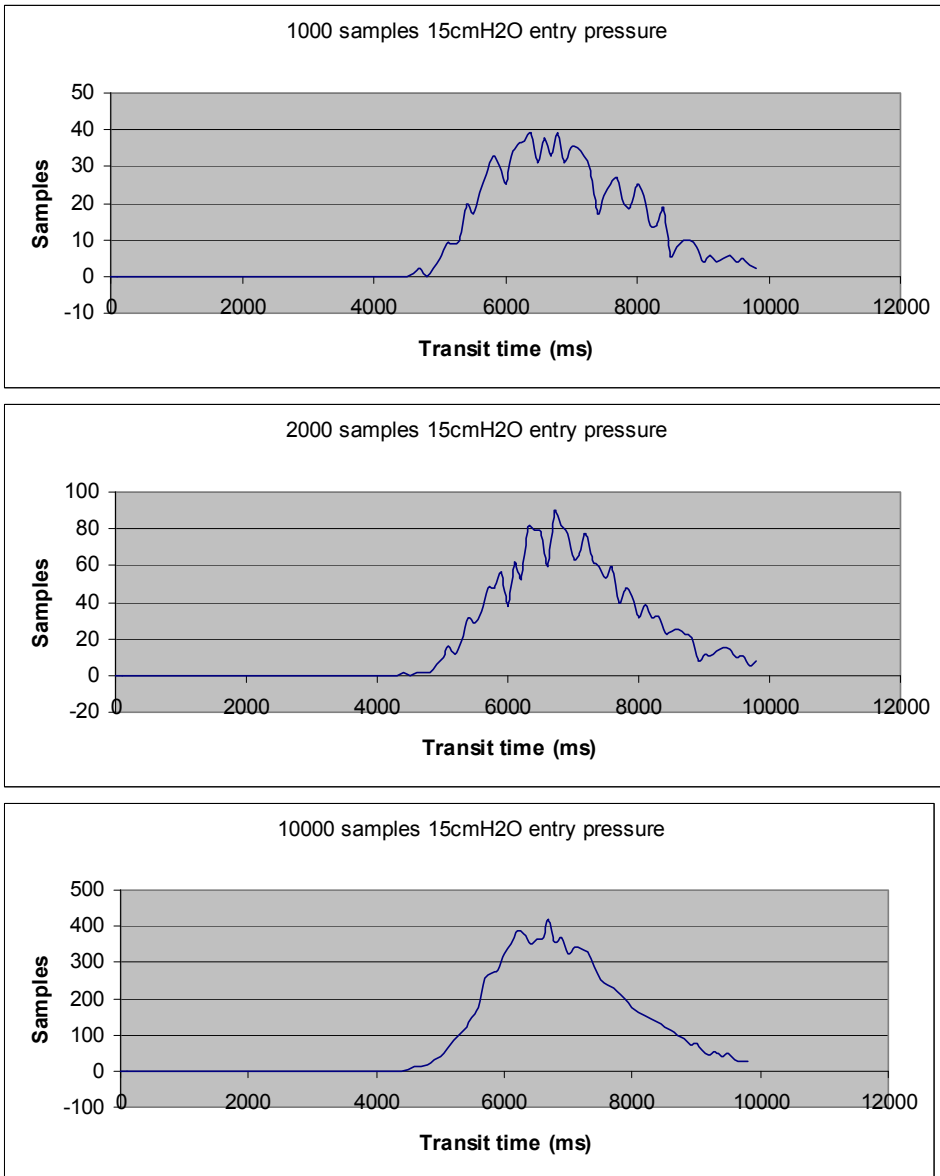


Figure 6: Transit times with different sample sizes

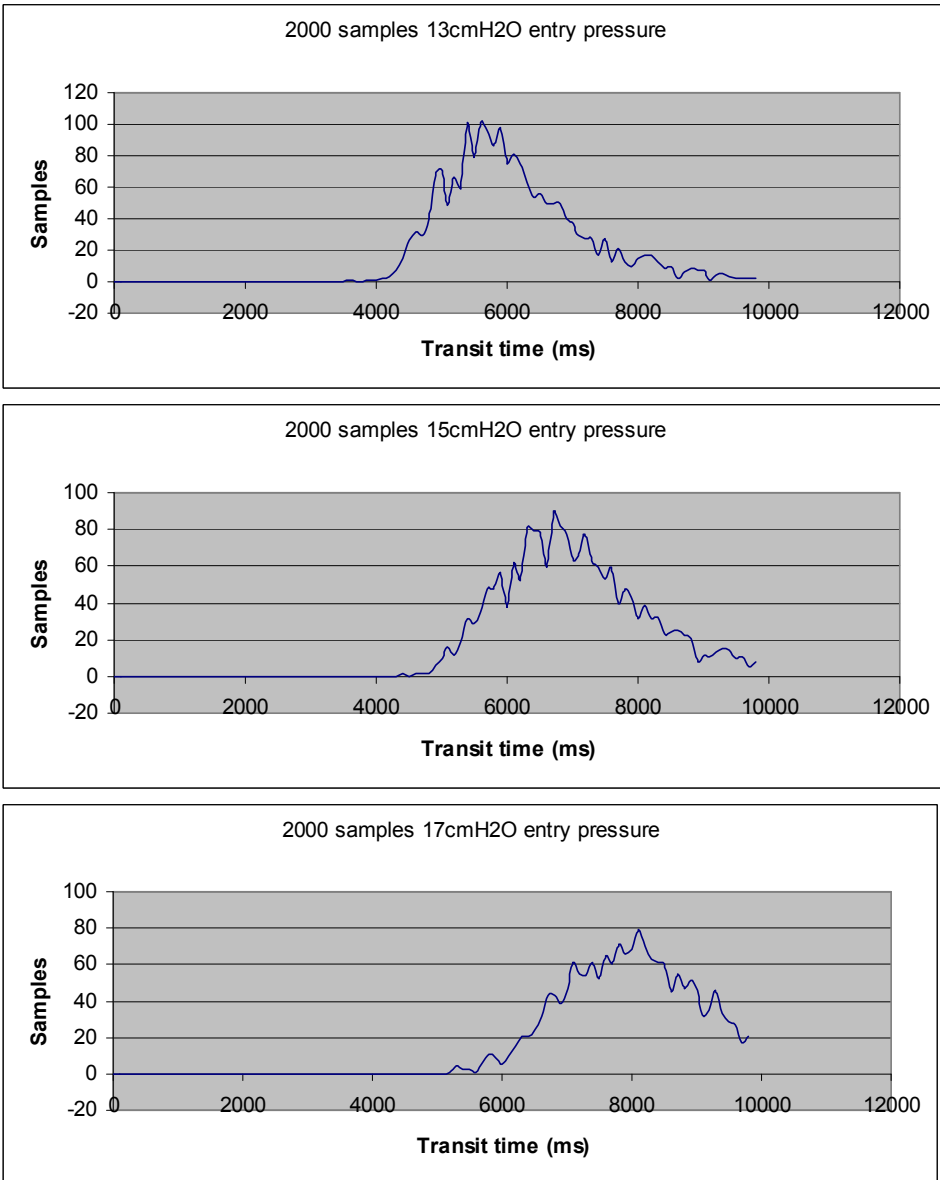


Figure 7: Transit times with different entry pressures

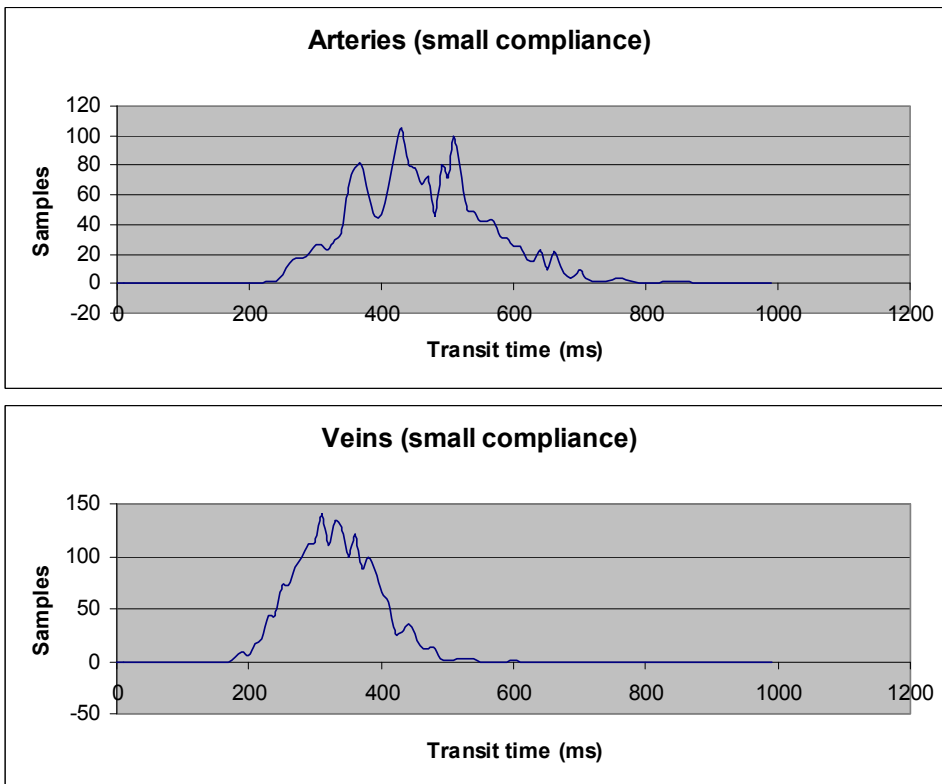


Figure 8: Transit time with small compliance conditions

entering the artery, ranging from 13 cmH₂O to 17 cmH₂O. When the entry pressure increases, based on Eq. (2), the exit pressure will increase. Since the pressure is on the fifth order, the pressure dropping across the vessel will decrease. The flow rate will decrease accordingly. It takes more time for the blood cells pass through the pulmonary circulation.

Wiggs presented the work in modeling neutrophil transit through the human pulmonary circulation in his dissertation [Wiggs (1994)], in which the pulmonary circulation was considered to be rigid for the modeling. **Figure 8** shows the results if we assign small values of compliances (less than 0.3). The distribution curves share the same pattern of the results from [Wiggs (1994)]. However, his dissertation reported the median value was 0.7 seconds for the distribution of arterial transit times and 0.8 seconds for venous transit times, which are higher than the results achieved in the present study. The main reason is that we are using different types of branching systems. Wiggs used a modified Horsfield branching structure

while we applied a Diameter-Defined Strahler System.

5 Conclusion

A stochastic simulation approach was introduced to simulate the blood flow in the hierarchical structure of a pulmonary circulation system without constructing the whole structure, and to calculate the transit time frequency distributions and the blood pressure outputs. In the stochastic model, the connectivity data between different levels of the pulmonary arteries and veins were converted into a probability matrix. The model was able to efficiently produce the transit time frequency distributions of the human pulmonary arterial and venous trees, respectively, and the whole pulmonary circulation.

References

1. Chiu, J. J.; Chien, S. (2011) Effects of disturbed flow on vascular endothelium: pathophysiological basis and clinical perspectives. *Physiol Rev.* 91: 327-87.
2. Fung, Y. C. (1996) *Biomechanics: Circulation*. New York: Springer-Verlag.
3. Fung, Y. C.; Sobin, S. S. (1969) Theory of sheet flow in lung alveoli. *J Appl Physiol* 26: 472-488.
4. Fung, Y. C.; Sobin, S. S. (1972) Pulmonary alveolar blood flow. *Circ Res* 30: 470-490.
5. Hopkins, S. R.; Belzbergm, A. S.; Wiggson, B. R.; McKenzie, D. C. (1996) Pulmonary transit time and diffusion limitation during heavy exercise in athletes. *Respir Physiol* 103: 67-73.
6. Hughes, J. M. B.; Morrell, N. W. (2001) *Pulmonary Circulation from Basic Mechanisms to Clinical Practice*. Imperial College Press, London.
7. Kassab, G. S.; Rider, C. A.; Tang, N. J.; Fung, Y. C. (1993) Morphometry of pig coronary arterial trees. *Am J Physiol* 265: H350-H365.
8. Huang, W.; Yen, R. T.; McLaurine, M.; Bledsoe, G. (1996) Morphometry of the Human Pulmonary Vasculature. *J Appl Physiol* 81(5): 2123-2133.
9. Huang, W.; Zhou, Q.; Gao, J.; Yen, R. T. (2011) A Continuum Model for Pressure-Flow Relationship in Human Pulmonary Circulation. *Molecular and Cellular Biomechanics*, 8: 105-122.

10. Lewis, M. L.; Caterinam, R. D., Giuntini, C. (1994) Distribution function of transit times in the human pulmonary circulation. *J Appl Physiol* 76: 1363-1371.
11. MacNee, W.; Martin, B. A.; Wiggs, B. R.; Belzberg, A. S.; Hogg, J. C. (1989) Regional pulmonary transit times in humans. *J Appl Physiol* 62: 844-850.
12. McLaurine, M. L. (1997) *Modeling studies of human pulmonary blood flow based on detailed anatomic and elasticity data*, Ph.D. dissertation, The University of Memphis.
13. Tawhai, M. H.; Clark, A. R.; Burrowes, K. S. (2011) Computational models of the pulmonary circulation: Insights and the move towards clinically directed studies. *Pulmonary Circulation*, 1: 224-238.
14. Wiggs, B. J. R. (1994) *Modeling neutrophil transit through the human pulmonary circulation*, Ph.D. dissertation, The University of British Columbia.
15. Yen, R. T.; Fung, Y. C.; Bingham, N. (1980) Elasticity of small pulmonary arteries in the cat. *J Biomech Eng* 102: 170-177.
16. Yuan, J. X. -J.; Garcia, J. G. N.; Hales, C. A.; Stuart, R.; Archer, S. L.; West, J. B. (eds.) (2010) *Textbook of Pulmonary Vascular Disease*. Springer, New York, NY.
17. Zavorsky, G. S.; Walley, K. R.; Russell, J. A. (2003) Red cell pulmonary transit times through the healthy human lung. *Experimental Physiology* 88: 191-200.
18. Zhuang, F. Y.; Fung, Y. C.; Yen, R. T. (1983) Analysis of Blood Flow in Cat's Lung with Detailed Anatomical and Elasticity Data. *J Appl Physiol: Respirat Environ Exercise Physiol* 55(4): 1341-1348.
19. Zhou, Q. (2005) *Human pulmonary circulation studied as an engineering system*, Ph.D. dissertation, The University of Memphis. .

Appendix: Algorithm used in the computational model

